Synthesis and Characterization of the Dansyltyrosine Derivatives of Porcine Pancreatic Colipase†

Jonathan C. McIntyre,‡ Friedhelm Schroeder,§,∥ and W. David Behnke*,‡

Department of Molecular Genetics, Biochemistry and Microbiology, College of Medicine, Department of Pharmacy and Medicinal Chemistry, College of Pharmacy, and Department of Pharmacology and Cell Biophysics, College of Medicine, University of Cincinnati, Cincinnati, Ohio 45267

Received May 12, 1989; Revised Manuscript Received October 23, 1989

ABSTRACT: Steady-state and time-resolved fluorescence techniques were used to study dansyltyrosine derivatives of porcine pancreatic colipase. Nitration, reduction, acylation, and dansylation reactions were utilized to synthesize two fluorescently labeled colipases: (*o*-aminodansyltyrosine 55 porcine colipase) (DNStyr55PC) and *o*-aminodansyltyrosine 59 porcine colipase (DNStyr59PC). DNStyr55PC was 200% active, while the DNStyr59 derivative maintained 80% activity in a pH stat assay. Emission spectra, lifetime analysis, acrylamide quenching, polarization, and anisotropy decay studies indicated that Tyr55 was located on the solvent-exposed surface of the protein, where the fluorophore experienced free rotation. Identical experiments done on DNStyr59PC indicated that Tyr59 was in a partially buried environment and the motion of the dansyl tyrosine group was hindered. The double-exponential decay of the fluorescence emission of *N*-acetyl-*o*-aminodansyltyrosine ethyl ester (DNStyr) and the DNStyr derivatives of colipase was investigated with pH, temperature, solvent, and emission-resolved-lifetime experiments. The existence of excited-state processes was eliminated in both pH and emission-resolved-lifetime experiments, whereas temperature studies indicated either a rotational isomer or a differential solvent quenching mechanism for multiple decay kinetics. These experiments also showed that DNStyr was a sensitive probe of solvent polarity and viscosity, but not of pH.

Pancreatic colipase anchors the enzymatically active form of lipase to its substrate, emulsified triglycerides (Canioni et al., 1977; Verger et al., 1977), thus reversing the inhibitory effects on lipase activity of both bile salt desorption (Chapus et al., 1975; Momsen & Brockman, 1976) and interface surface denaturation. This anchoring requires the binding of colipase to an oil/water interface; making colipase–lipase a paradigm for biological molecules that utilize phase interactive surface catalysis. The binding of colipase to the interface is thought to occur at a specific site on the protein molecule as evidenced by small-angle neutron scattering (Charles et al., 1980) and analytic ultracentrifugation data (Charles et al., 1975). UV spectrophotometry (Sari et al., 1975), circular dichroism (Donner et al., 1976), ^{1}H NMR[1] (Cozzone, 1976; Wieloch & Falk, 1978), and photochemically induced dynamic nuclear polarization (photo-CIDNP) (Canioni et al., 1980a; Cozzone et al., 1981) studies performed on colipase and colipase–micelle complexes formed with sodium taurodeoxycholate (a model system for bile salt emulsified fat droplets) have provided evidence that one or more tyrosyl residues of the colipase molecule are involved in micelle binding. In addition, detailed analysis of perturbations in NMR titration profiles and chemical shifts reveals a specific interaction of one histidyl, one tyrosyl, and to a lesser extent another tyrosyl residue with micelles (Canioni & Cozzone, 1979a,b; Canioni et al., 1980b). The interpretation of these data suggests that the protein folding of colipase brings into juxtaposition regions of the primary structure rich in hydrophobic residues, creating a hydrophobic loop domain containing six and possibly all seven aromatic residues in the protein. This hydrophobic domain is postulated to contain the peptide regions 50–60, Ser-Ala-Phe-Thr-Leu-Tyr-Gly-Val-Tyr-Tyr-Lys; 84–88, Phe-Gly-Ile-Cys-His; and possibly 29–37, Gln-His-Asp-Thr-Ile-Leu-Ser-Leu-Leu.

Further evidence supporting the hydrophobic domain theory comes from spectrofluorometric studies on equine colipase, which has a tryptophan at position 52 instead of phenylalanine in the porcine protein. Acrylamide, Cs^+ and I^- quenching in the absence and presence of cmc levels of taurodeoxycholate (TDOC) showed that Trp52 is a surface residue that becomes shielded from quenching when the protein binds TDOC micelles (McIntyre et al., 1987). Excluding the possibility of conformational changes brought about by TDOC binding, these data suggest that Trp52 is located in or near the "lipid recognition site" and further validate the observation that residues 50–60 are located in a hydrophobic loop domain. More detailed evidence comes in the form of preliminary 2D NMR NOESY experiments (R. Stark, personal communication) that may indicate a close proximity between residues

† Supported in part by NIH Grants GM 31651 and DK41402 to F.S. A previous paper has been presented (McIntyre et al., 1989).

* To whom correspondence should be addressed.

‡ Department of Molecular Genetics, Biochemistry and Microbiology, College of Medicine.

§ Department of Pharmacy and Medicinal Chemistry, College of Pharmacy.

∥ Department of Pharmacology and Cell Biophysics, College of Medicine.

[1] Abbreviations: NMR, nuclear magnetic resonance; NOESY, nuclear Overhauser effect spectroscopy; 2D, two-dimensional; HPLC, high-pressure liquid chromatography; IR, infrared spectroscopy; cmc, critical micellar concentration; DEAE, diethylaminoethyl; NEM, *N*-ethylmaleimide; TNM, tetranitromethane; dansyl (DNS), 5-(dimethylamino)-1-naphthalenesulfonyl; Acrylodan, 6-acryloyl-2-(dimethylamino)naphthalene; Prodan, 6-propionyl-2-dimethylnaphthalene; dimethyl-POPOP, 1,4-bis[4-methyl-5-phenyl-2-oxazolyl]benzene; DNStyr55PC, *o*-aminodansyltyrosine 55 porcine colipase; DNStyr59PC, *o*-aminodansyltyrosine 59 porcine colipase; NH_2tyr55PC, *o*-aminotyrosine 55 porcine colipase; DNStyr, *N*-acetyl-*o*-aminodansyltyrosine ethyl ester; *N*-term PC, *N*-dansyl-Gly 1 porcine colipase.

0006-2960/90/0429-2092$02.50/0

Tyr55 and His88 indicative of a foldover to form a hydrophobic aromatic region. The earlier NMR work had identified tyrosyl residues 58 and 59 to be the surface-exposed residues (Wieloch & Falk, 1978; Canioni & Cozzone, 1979a). In contrast, the preliminary data of Stark and the chemical modification data presented by McIntyre et al. (1987) identify Tyr55 as being one of the surface tyrosines.

Herein are assessed the roles of the tyrosine residues in the lipid recognition site, using a strategy of nitration, reduction, and dansylation of tyrosine to generate fluorescent probes of tyrosines 55 and 59. The properties of these two derivatives of colipase were examined by multifrequency (1–250 MHz) phase and modulation spectrofluorometry in an attempt to assign clearly the surface tyrosines of porcine colipase.

Materials and Methods

Proteins and Reagents. Porcine pancreatic lipase was kindly provided by M. Rovery and colleagues from the Centre de Biochimie et de Biologie Moleculaire du Centre National de la Recherche Scientifique, Marseilles, France. Porcine colipase was isolated according to the procedure of Chapus (Chapus et al., 1981). Acetone powders of porcine pancreas were generated from fresh tissue (Kahns Meats; Cincinnati, OH) in our laboratory. Tetranitromethane from Aldrich Chemical (Milwaukee, WI) was extracted with quartz distilled water (5×) prior to use. Sodium taurodeoxycholate (recrystallized in ethanol after activated charcoal treatment), *N*-acetyl-nitrotyrosine ethyl ester dansyl chloride, and *N*-ethylmaleimide were all purchased from Sigma Chemical (St. Louis, MO). Sodium dithionite was purchased from Matheson Coleman and Bell (Norwood, OH). HPLC grade solvents and dansylated amino acid standards were obtained from Pierce Chemical (Rockford, IL). Sephadex G-25, Sephadex G-50, and DEAE-Sephacyl were purchased from Pharmacia (Piscataway, NJ). Acrylamide was obtained from Bio-Rad (Richmond, CA) and recrystallized twice in ethanol–water. All other reagents were of the highest quality available.

Colipase Activity and Characterization. Lipase–colipase enzyme activity was measured by use of a tributyrylglycerol emulsion/4 mM TDOC assay (Chapus et al., 1981) monitored with a Radiometer (Copenhagen, Denmark) pH stat. Colipase activity is observed as the increase in lipase activity attributed to the addition of colipase to the assay system. The kinetic parameters V_{max} and K_m are not obtained as the concentration of the insoluble substrate cannot be varied. Therefore, the activity of modified colipases was determined as a percent of standard colipase activity. Protein concentration was determined by absorbance $E_{m280nm} = 4200\ M^{-1}\ cm^{-1}$ for unmodified porcine colipase and by the method of Lowry for modified protein. The extent of modification after reaction with tetranitromethane was calculated by absorbance, $E_{M381nm} = 2200\ M^{-1}\ cm^{-1}$ (Sokolovsky et al., 1966). For the dansylated derivatives of colipase, dansyl-NH-tyrosine content was determined by absorbance $E_{M350nm} = 3980\ M^{-1}\ cm^{-1}$ (Johnson et al., 1978).

Synthesis and Characterization of N-Acetyl-o-amino-dansyl-L-tyrosine Ethyl Ester. *N*-Acetyl-*o*-nitro-L-tyrosine ethyl ester in 40% ethanol was reduced to the amino form with a 16-fold molar excess of $Na_2S_2O_4$ at room temperature for 2 h. The solvent was removed by vacuum rotary evaporation, and the organic products were separated from salt by three extractions with butanol. The butanol was removed by vacuum evaporation, and the remaining aminotyrosine was dissolved into 0.1 M NaOAc and 0.9% NaCl, pH 5.0, buffer. The buffered solution was reacted with 10-fold molar excess of dansyl chloride at 65 °C in the dark for 24 h with stirring. The yellowish orange aqueous layer was removed by centrifugation. The remaining dark orange oil was collected and washed three times with distilled water and then dried with acetone. The reaction products were separated by HPLC on a Waters system with a Waters semiprep C-18 column (1.0 × 25 cm). Separation of four peaks corresponding to aminotyrosine, dansylamide, dansylsulfonic acid, and dansyltyrosine was achieved with isocratic conditions utilizing a 50% acetonitrile/50% double-distilled H_2O solvent system. The peaks were tentatively identified on TLC by comparison to the known standards; dansylsulfonic acid, dansylsulfonamide, and *N*-acetyl-*o*-amino-L-tyrosine ethyl ester. Thus, the dansyltyrosine product could be determined without having a standard by an elimination process. Thin-layer chromatography experiments were done in duplicate by utilizing two different solvent systems: hexane:chloroform:methanol (3:6:1) and butanol:acetic acid:water (1:5:2). The support was silica gel 60 F-254 0.25-mm precoated sheets (E. Merck, Darmstadt, Germany), and the spots were visualized under a UV lamp. The HPLC peak corresponding to dansyltyrosine was collected, reinjected, and finally characterized by IR and TLC. Infrared absorbance was measured on a 1420 IR spectrometer (Perkin-Elmer, Norwalk, CT), and the sample was prepared for scanning by the KBr pellet technique. The product showed only one spot on TLC and characteristic carbonyl (1700 cm^{-1}), hydroxyl (3500–3100 cm^{-1}), and sulfonyl (1355 and 1170 cm^{-1}) bands in the IR spectrum. The pure compound containing carbonyl, hydroxyl, and sulfonyl functional groups could only be *N*-acetyl-*o*-nitro-L-tyrosine ethyl ester.

Instrumentation. UV and visibile absorbance measurements were made on a Cary 15 scanning spectrophotometer (Varian, Monrovia, CA). Steady-state spectrofluorometric measurements were obtained on a MPF-44A equipped with a DCSU-2 corrected spectra unit (Perkin-Elmer). Time-resolved fluorescence experiments were made on a SLM 4800 subnanosecond spectrofluorometer modified to a 1–250-MHz multifrequency capability (Nemecz & Schroeder, 1988). A Liconix He/Cd laser was used as the light source with an emission intensity at 325 nm that was sinusoidally modulated with a Pockels cell. The emission was observed in the L format through a Janos GG-375 cut-off filter for both lifetime and differential polarization experiments (Nemecz & Schroeder, 1988; Sweet et al., 1987; Schroeder et al., 1987; Fischer et al., 1985). The data were collected by an IBM PC utilizing ISS-01 and ISS-187 software (ISS Instruments Inc., Urbana, IL).

Lifetime Data Acquisition and Calculation. Fluorescence lifetimes were determined by using the phase and modulation technique (Nemecz & Schroeder, 1988; Schroeder et al., 1987; Sweet et al., 1987; Fischer et al., 1985). Data were collected at 8–16 modulation frequencies (15–170 MHz) with respect to the reference fluorophore dimethyl-POPOP in absolute ethanol (lifetime of 1.45 ns) (Lakowicz et al., 1981). The excitation polarizer was set at 0°, and the emission polarizer was set at the magic angle of 55° to eliminate Brownian motion as a determinant of apparent lifetime. Data were collected and analyzed by the aforementioned ISS-01 and ISS-187 software. Lifetime analysis was performed by either a nonlinear least-squares analysis (Lakowicz et al., 1984) or a Lorentzian continuous distribution analysis (Fiorini et al., 1987; Caceri & Cacheris, 1980) for a one-, two-, or three-component fit. Lorentzian continuous distribution analysis was favored for this work due to the added dimension of measuring width distributions. The ability to measure width distribution gives additional evidence for the homogeneity of

a particular emitting species, which is very informative in protein studies (Alcala et al., 1987a,b). Possible conformational changes, local fluctuations, and segmental motions can be monitored with such a parameter. The reduced χ^2 parameter was utilized to judge quality of fit. For both nonlinear least-squares and distribution analysis the ISS-187 program minimized the reduced χ^2 defined by

$$\chi^2 = S\{[(P_m - P_c)/S_p]^2 + [(M_m - M_c)/S_m]^2\}/[(2n - f - 1)] \quad (1)$$

where c and m indicate the calculated and measured values, respectively, of phase (P) and modulation (M), n is the number of frequencies employed (8–16 frequencies; 15–170 MHz), f is the number of free parameters and Sp and Sm are the standard deviations of each phase and modulation determination, respectively. In all analyses presented, a two-component fit gave 2–3-fold improvement in χ^2 over a one-component fit. A three-component fit gave χ^2 values similar to those of a two-component fit; however, the third component was a negligible fraction of the total intensity. Emission-resolved lifetimes were obtained with use of either a monochromator or a series of cutoff filters to select the proper emission wavelength. Low signal to noise ratios due to intensity limitations dictated the use of cutoff filters instead of a monochromator for several experiments.

Differential Polarization Measurements. Differential phase and modulation ratio experiments were used to calculate both static polarization values and time-resolved anisotropies (Nemecz & Schroeder, 1988; Wood et al., 1987; Schroeder et al., 1987). Data were collected by ISS-01 software utilizing the differential polarization program and calculated by the Rotational Least-Squares Analysis program, which fits the data to

$$F(t) = \sum_j [1 + ar(t)]i(t) \quad (2)$$

where the eqs 3 and 4 represent $r(t)$ and $i(t)$, respectively. The

$$r(t) = \sum_l [1 + ag_l \exp(-t/R_l)] \quad (3)$$

$$i(t) = \sum_i [f_i \exp(-t/T_i)] \quad (4)$$

following indices represent constants that depend upon the nature of the sample being observed: j is the number of species present, l indicates the number of rotational components for each species, and i represents the number of lifetime components for each species. T_i and f_i are the values of emission lifetime and fractional intensity, respectively. The summation of the fractional contributions g_l is the limiting anisotropy. The rotational correlation times are represented by R_l.

From this, it is possible to calculate anisotropy decay parameters from one set of data in several different manners depending upon the rotational model assumed. We have used three models for anisotropy decay depending upon the species being analyzed, isotropic, anisotropic, and hindered. The respective equations that define these models are the following (Lakowicz et al., 1985):

for an isotropic rotator

$$r(t) = r_0 \exp(-t/R) \quad (5)$$

for an anisotropic rotator

$$r(t) = r_0[g_1 \exp(-t/R_1) + g_2 \exp(-t/R_2)] \quad (6)$$

and for a hindered rotator

$$r(t) = (r_0 - r_{inf}) \exp(-t/R) + r_{inf} \quad (7)$$

In eq 7 r_{inf} represents the limiting anisotropy at infinite time.

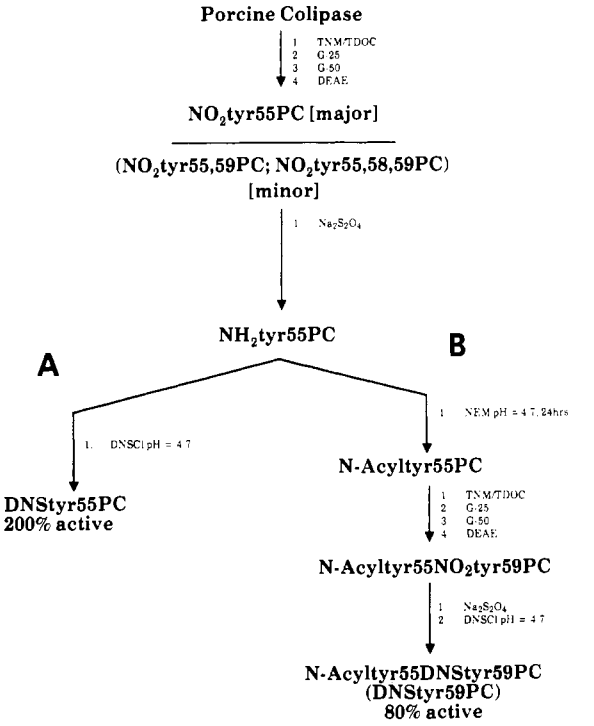

FIGURE 1: Chemical modification flow chart for nitration, reduction, and dansylation of porcine pancreatic colipase. All reactions were carried out at room temperature. Nitration was accomplished in a 100 mM NaCl, 5 mM $CaCl_2$, and 50 mM Tris-HCl, pH 8.0, buffer. Dansylation and acylation were done in a 50 mM NaOAc, pH 4.7, buffer, while reduction reactions were carried out with a 16-fold molar excess of $Na_2S_2O_4$ in 50 mM Tris-HCl and 5 mM $CaCl_2$, pH 9.0, buffer.

The reduced χ^2 values for differential polarization minimizations are not necessarily an absolute measure of goodness of fit but are useful for component fit comparisons. Abbreviations for the the models presented are the following: R, isotropic rotator; $2R$, anisotropic rotator; and R,r_{inf}, hindered rotator.

Absolute Quantum Yield Determination. The absolute quantum yield was determined as described in Prendergast et al. (1983) by utilizing

$$Q_{Un}/Q_K = (F_{Un}/F_K)(A_K(ex)/A_{Un}(ex)) \quad (8)$$

In eq 8 Q is the absolute quantum yield, F is the fluorescence emission, and A is the absorbance at the excitation wavelength. The known compound (K) used in the determination was dansylamide, with a value of 0.1 for Q_K as given in Cantor and Schimmel (1980). Fluorescence emission was determined for both known and unknown (Un) with the same instrument settings. Values for A(ex) were determined as an average of three readings.

Results

Nitration, Reduction, and Dansylation of Porcine Pancreatic Colipase. Nitration of colipase was accomplished by the method of DeCaro (DeCaro et al., 1983), specifically by using the conditions of method III, low TNM excess in the presence of TDOC micelles. After the reaction had run its time course (1 h), the products were subjected to the following series of columns: G-25, G-50, and DEAE as shown in Figure 1. DEAE chromatography allowed for the isolation of three chemically modified and one unmodified form of colipase. The three modified forms represent the modification of the three tyrosines with the order of reactivity 55 > 59 > 58, as determined by sequence analysis (DeCaro et al., 1983; McIntyre et al., 1987). The specificity and extent of nitration was

checked by protein concentration assays and visible extinction for nitrotyrosine, as described under Materials and Methods. Characteristic visible CD patterns also supported the fidelity of nitration reactions (DeCaro et al., 1984). The lone modified Tyr55 colipase was further modified by complete reduction to aminotyrosine with $Na_2S_2O_4$ (Sokolovsky et al., 1967), and after thorough dialysis against 0.1 M sodium acetate/0.9% sodium chloride, pH 4.7, the aminotyrosine residue was reacted with dansyl chloride, pH 4.7 (reaction pathway A in Figure 1), as described by Cardin et al. (1982). This fluorescent derivative of colipase was shown to have 200% of the activity of the native protein. Colipase activity, which is the stimulation of lipase activity due to the addition of colipase, was measured by pH stat assay utilizing tributyrin as substrate. It was shown by Kenner and Neurath (1971) that treatment of trypsin with dansyl chloride at pH 5.0 did not incorporate any dansyl into the protein. Only after nitration with TNM and reduction with $Na_2S_2O_4$ could any dansyl be incorporated into trypsin at pH 5.0. A similar experiment performed on colipase (described below) showed that the dansylation reaction run at pH 4.7 was specific for the *o*-amino group of aminotyrosine.

To generate a probe to monitor exclusively the role of Tyr59 in lipid recognition and binding, we followed the combined procedures of DeCaro and Cardin to synthesize NH_2Tyr55PC. This form of colipase was then reacted with a 10-fold molar excess of *N*-ethylmaleimide at pH 4.7 for 24 h at room temperature (reaction pathway B). NEM is a well-known sulfhydryl reagent that has also been shown to be reactive toward histidine and lysine residues (Smyth et al., 1960). However, the latter reactions are sluggish and require the pH of the reaction to be run near the pK_a of the reacting species. Thus, fixing the pH of the reaction at 4.7 makes it highly improbable that any side reactions with Lys or His would occur. Colipase does not contain any free sulfhydryls; therefore, the reaction should be specific for aminotyrosine. Although the specificity of the reaction can be controlled by reaction conditions, the extent of modification must also be considered as the blocking reaction must proceed to 100% completion before further reactions. The extent of NEM modification was determined by reacting the product of the NEM–colipase reaction with dansyl chloride at pH 4.7 (unpublished results). This experiment would show if NEM completely blocked the *o*-amino group of aminotyrosine and if any side reactions occur during dansylation. No dansyl was incorporated under these conditions, showing that the amino group was completely blocked and that the dansylation reaction was specific when run at pH 4.7. The *N*-acylamino Tyr55 derivative was then resubjected to nitration. Only one nitrated form of colipase was identified from DEAE chromatography (Tyr59). This species was shown to contain 0.97 (±0.5) mol of NO_2/mol of protein by Lowry protein assay and chromophore spectrophotometric extinction (Sokolovsky et al., 1966). This derivative was then further processed by reduction and dansylation (as described earlier) and shown to possess 80% of the activity of unmodified colipase.

Characterization of the Microenvironments of DNStyr55 and DNStyr59. (a) Emission Spectra of Dansyltyrosine, DNStyr55PC, and DNStyr59PC. The emission spectra of DNStyr55PC, DNStyr59PC, and DNStyr are presented in Figure 2. The corrected emission spectrum of DNStyr55PC (panel A) shows a broad maximum centered at 550 nm with a half-height bandwidth of 80 nm. An emission maximum of 550 nm is highly red shifted for a fluorophore that is a naphthalene derivative (Prendergast et al., 1983; Macgregor & Weber, 1986; Cantor & Schimmel, 1980), suggesting that the dansyl group is in a polar environment, surface exposed, and solvent accessible. The DNStyr59PC derivative of porcine colipase has an emission maximum at 520 nm. The shape of the spectrum is also very broad with a half-height bandwidth of 94 nm. The dansyl group attached at Tyr59 is less surface exposed than Tyr55, by emission maximum comparison, but still in a fairly polar environment. The emission spectra of DNStyr in buffer and propylene glycol are presented in panel B of Figure 2. In buffer the emission maximum is 526 nm and in propylene glycol, 510 nm; both spectra are very broad.

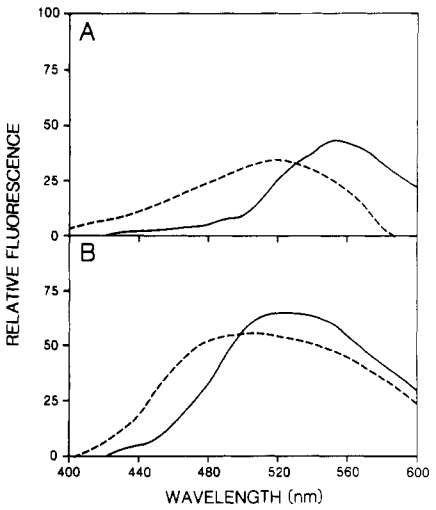

FIGURE 2: Fluorescence emission spectra of DNStyr and DNStyr derivatives of colipase. The instrument was set at an excitation wavelength of 325 nm with 8-nm slit widths for both excitation and emission. The spectra were taken in the corrected mode. The solution was a 0.05 M K_2HPO_4, pH 7.4, buffer, and all spectra were measured at room temperature. (A) (—) 0.56 mg/mL DNStyr55PC [buffer]; (---) 0.68 mg/mL DNStyr59PC [buffer]. (B) (—) DNStyr [buffer]; (---) DNStyr [propylene glycol].

Table I: Analysis of Fluorescence Emission Decay of DNStyr and DNStyr Derivatives of Colipase[a]

sample	$C[1]$	$W[1]$	$F[1]$	$C[2]$	$W[2]$	$F[2]$	χ^2
DNStyr55PC	11.8	0.05	0.74	1.3	0.41	0.26	26.1
DNStyr59PC	9.9	0.05	0.68	1.5	0.49	0.32	23.2
DNStyr/[buffer]	13.1	0.05	0.90	2.5	0.34	0.10	2.1
DNStyr/[propylene glycol]	15.2	0.29	0.95	0.7	0.16	0.05	24.3

[a] C is the center of the distribution in nanoseconds, F is the fractional intensity, and W is the width at half-height of the distribution in nanoseconds.

The absolute quantum yield of DNStyr55PC is 0.16 and is 0.12 for DNStyr59PC. These are slightly higher than the value of 0.10 for DNS (Cantor & Schimmel, 1980). The smaller value of Q for DNStyr59PC combined with its blue shifted emission maximum relative to DNStyr55PC would suggest that the dansyl group at Tyr59 may be slightly buried, causing its emission to be quenched by internal groups.

(b) Lorentzian Continuous Distribution Lifetime Analysis of DNStyr55PC, DNStyr59PC, and DNStyr. Panels A–D of Figure 3 show the distributions of the lifetimes for DNStyr55PC, DNStyr59PC, DNStyr/buffer, and DNStyr/propylene glycol as calculated by a Lorentzian continuous distribution analysis. The numerical parameters derived from these calculations are presented in Table I. Panel A shows the lifetime distribution for DNStyr55PC, which has a two-component fit. The first fraction comprising 74.1% of the fluorescence ($F[1]$) is centered at 11.7 ns ($C[1]$) with a half-height width ($W[1]$) of 0.05 ns. A value of 0.05 ns for $W[1]$ suggests that the emitting species represented by com-

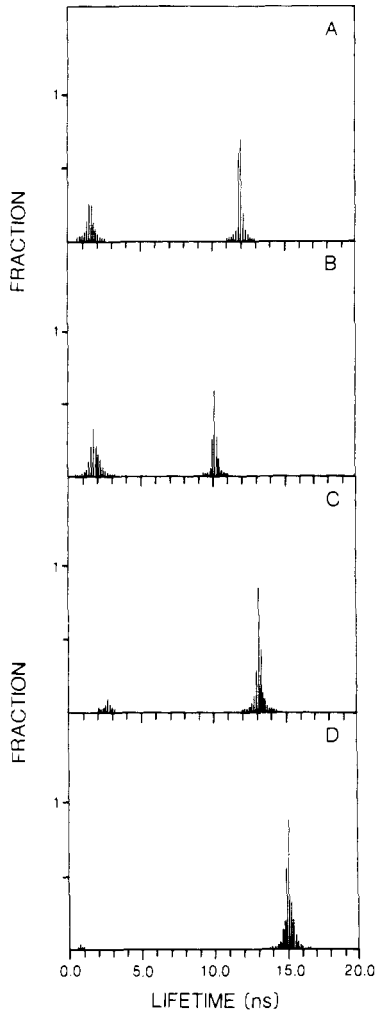

FIGURE 3: Lorentzian continuous distribution analysis of the fluorescence lifetime of DNStyr and DNStyr derivatives of colipase. All measurements were made at 24 °C; the buffered solution was 0.05 M K_2HPO_4, pH 7.4. The concentration of the sample was diluted so as to have an $OD_{325nm} < 0.20$. (A) DNStyr55PC, [buffer]. (B) DNStyr59PC, [buffer]. (C) DNStyr, [buffer]. (D) DNStyr, [propylene glycol].

ponent 1 is highly homogeneous. The center of the second distribution is at 1.3 ns with a broader width of 0.40 ns that represents 25.9% of the fluorescence. The broad width of $C[2]$ is indicative of more heterogeneous population of emitting species. The lifetime distribution analysis of DNStyr59PC (panel B) also has a two-component fit with $C[1]$ shifted to a smaller value of 9.9 ns as compared to that of DNStyr55PC. The width is the same with a value of 0.05 ns, and the fraction is smaller at 67.8% of the fluorescence. The second component is centered at 1.5 ns with a broader width of 0.49 that comprises 32.2% of the fluorescence. The $C[1]$ value for DNStyr in buffer (panel C) is 13.1 ns, which is similar to lifetimes obtained for dansyl attached to Lys or Cys (Cantor & Schimmel, 1980), with $W[1] = 0.05$ ns and $F[1] = 0.90$. The second lifetime component is centered at 2.5 ns with a width of 0.3 ns contributing 9.9% of the intensity. In going from buffer to propylene glycol the $C[1]$ component of DNStyr shifts to 15.1 ns, the width increases to 0.29 ns, and the fraction increases to 94.8%. The second component, which comprises 5.2% of the intensity, is centered at 0.74 ns with a half-height width of 0.16 ns.

From Table I it can be seen that many similarities exist between the four distributions. All have two components, $C[1]$ being approximately 12 ± 3 ns and $C[2] = 1.5 \pm 1$ ns. The width of the first component is 0.05 ns in all cases except

Table II: Differential Polarization and Anisotropy Decay Parameters[a]

sample	P	fit	R	r_{inf}	g	χ^2
DNStyr55PC	0.055	$2R$	1.03		0.098	4.0
			4.72		0.113	
		R,r_{inf}	1.26	−0.003		7.4
DNStyr55PC (20% sucrose)	0.096	$2R$	1.88		0.093	25.1
			9.56		0.068	
		R,r_{inf}	2.02	0.042		24.4
DNStyr59PC	0.105	$2R$	0.66		0.189	12.7
			11.97		0.135	
		R,r_{inf}	1.09	0.047	0.099	12.0
N-termPC	0.122	$2R$	0.98		0.099	2.2
			13.36		0.138	
		R,r_{inf}	2.28	0.061		3.0
DNStyr	0.015	R	1.56		0.132	131.4
		R,r_{inf}	2.35	−0.002		28.1

[a] All experiments were performed at 24 °C in a 0.5 M K_2HPO_4, pH 7.4 buffer. P is the polarization, R is the rotational relaxation time, r_{inf} is the limiting anisotropy at times greater than the emission lifetime, and g is the sum of the fractional contributions to depolarization. Fit refers to the model used to calculated anisotropy decay: R is the isotropic rotator model; $2R$ is the anisotropic rotator model; R,r_{inf} is the hindered rotator model.

DNStyr/propylene glycol, and the width of the second component is always much larger (near 0.4 ns) except again with DNStyr in propylene glycol. The size of the widths of the distribution analyses suggests that the shorter lifetime component is more heterogeneous than the first component.

(*c*) *Polarization and Anisotropy Decay.* Static polarization and anisotropy decay measurements can be used to reveal the rotational dynamics of a fluorophore. The dynamic properties of the dansyl derivatives of colipase were examined by using multifrequency differential phase fluorometry as shown in Table II. There were two reasons for measuring anisotropy decays in this system. The first was to be able to describe the environments of tyrosines 55 and 59 with greater resolution. This would be accomplished by comparing the corresponding anisotropy decay values for DNStyr55PC, DNStyr59PC, and DNStyr. However, differences in anisotropy values where only a single probe is present can be due to different orientations of the emission dipole and protein major axis. Since the probes are located relatively close to one another in the primary sequence, it is probable that the former interpretation is more valid. The other was to determine whether the fluorophore rotates on the time scale of the lifetime emission. The latter was derived from a model of tryptophan fluorescence, which suggests that multiexponential emission decay kinetics may be described by flexible rotamers that sample different microenvironments on the time scale of emission, thus experiencing different quenching events (Ross et al., 1981). To investigate both of these concerns, anisotropy decays and polarization were measured for DNStyr55PC, DNStyr59PC, DNStyr, and N-termPC (colipase modified at the N-terminal with dansyl chloride).[2] These measurements were also taken for DNStyr55PC in 20% sucrose, which was done to increase the viscosity of the medium, causing the tumbling rate of the protein to slow down but changing the fluorophore rotation only marginally (Ross et al., 1986). The anisotropy decay data from this experiment should reflect this by showing a considerable increase in one relaxation time over another. Therefore, this experiment should determine whether our models can resolve the proper rotational components. Several models for the decay of anisotropy were used to calculate the rotational dynamics of the samples in question. The models

[2] J. C. McIntyre, unpublished observations.

depend on the number of fluorescent species and the number of rotational motions that describe each species. Irrespective of the model, the value of r_0 (eq 5–7) was allowed to vary throughout minimization.

Polarization measurements determine the displacement of a fluorophore between the time of absorption and emission. Steady-state measurements of polarization (P) for a fluorophore attached to a protein are dependent upon the movement of both the fluorophore and the protein. Assuming that modification of colipase does not effect protein tumbling, differences in the value of P for dansyl-modified colipases can be attributed to local fluorophore depolarization. The steady-state polarization of DNStyr55PC is 0.055, which is only 55% of the value of DNStyr59PC, $P = 0.105$. The model compound DNStyr represents the free rotation of dansyl attached to tyrosine and had a $P = 0.015$. This suggests that the dansyl group at position 59 is more hindered than at position 55 and that position 55 is free to rotate by comparison to the model compound. These conclusions are based on indirect measurements of the rotation of the fluorophore. Direct measurements were obtained through the calculation of anisotropy decays.

The anisotropy decay fit designated $2R$ (eq 6) represents the model for an anisotropic rotator. This method generates two rotational relaxation times with two corresponding (g) values and was utilized in an attempt to resolve correlation times for the dansyl group and for the protein. This model produces reasonably acceptable values for DNStyr55PC with $R_1 = 1.0$ ns and $R_2 = 4.7$ ns. The rotational rate R_1 represents the rotation of the fluorophore, while R_2 represents the tumbling of the entire molecule. Altering the viscosity of the solvent increased the value of R_1 by 0.85 ns, but more significantly, the value of R_2 increased by 4.84 ns. The ability to resolve correlation times for fluorophore and protein would suggest that the anisotropic rotator model can effectively describe the anisotropy decay of DNStyr59PC. The anisotropic rotator model did not properly describe the anisotropy decays of DNStyr59PC or N-termPC.

The hindered rotator model [designated, fit R, r_{inf} (eq 7)] is applied to anisotropy decay data when it is presumed that the fluorophore angular range of rotational motion is limited due to environment. The anisotropy will not decay to zero if the rotational motions of the fluorophore are hindered. This is determined by measuring the limiting anisotropy at times much longer than the lifetime. The r_{inf} value has been described as the measure of an energy barrier that prohibits free rotation (Lakowicz, 1983). By application of the wobbling-in-cone theory (Munro et al., 1979) utilizing the equation $\theta_{max} = -\cos - 1(^1/_2\{[1 + 8(r_{inf}/r_0)^{1/2}]^{1/2} - 1\})$, the approximate amplitude of the internal rotation can be estimated. From this relationship it can be seen that greater values of r_{inf} represent more hindered fluorophore motion. With our experimental procedures, we are confident of resolving an accurate singular hindered rotation. The single R (rotational relaxation time) and r_{inf} (infinite anisotropy) values obtained from these analyses are weighted averages of both fluorophore and the entire molecular depolarization. Assuming that chemical modification of colipase does not alter the rotational properties of the molecule, the average r_{inf} value indicates changes in local fluorophore environment when compared to other modified colipases.

When the value of r_{inf} is greater than zero, hindrance is occurring in the system (Lakowicz et al., 1983). The presence of a hindered rotation for DNStyr in buffer would not be expected and was borne out by a negative value for r_{inf}. The negative value of r_{inf} for DNStyr55PC is in agreement with other fluorescence data presented herein, which suggests that Tyr55 is on the surface of the molecule and is free to rotate. This also indicates that the anisotropic rotator model gives a better description of the anisotropy decay for DNStyr55PC than the hindered rotator model. In contrast, a hindered rotation of DNStyr59 is observed by a 0.042 value for r_{inf}, which is in agreement with other physical data that indicate a partially buried conformation for Tyr59. On the whole, the rotational correlation times obtained from either rotational model analysis suggest that the rotation of the fluorophore is near 1–2 ns in both DNStyr55PC and DNStyr59PC. This would permit the fluorophore to experience multiple microenvironments on the time scale of both lifetime components.

Model Compound Studies. To characterize the fluorescence properties of the dansyl derivatives of porcine pancreatic colipase, we compared the spectral properties of the modified proteins to the model compound, dansyltyrosine. The continuous distribution analyses of the lifetime emission of DNStyr, DNStyr55PC, and DNStyr59PC were best fit with a double-exponential decay or component distribution. This would suggest that *o*-aminodansyl derivatives of tyrosine exhibit complex physical parameters. A detailed physical description of the photophysics of dansyltyrosine and dansyltyrosine-labeled proteins has not yet been established. Work presented herein utilizing models developed in studies of tyrosine, tryptophan, and other fluorophore systems (Beechem & Brand, 1985) will attempt to elucidate the complex nature of the emission decay of these molecules as well as characterize the usefulness of dansyltyrosine as a reporter group.

(*a*) *Effect of pH on the Fluorescence Properties of DNStyr55PC, DNStyr59PC, and DNStyr.* One mechanism by which a single fluorophore could exhibit double-exponential decay is through the existence of excited-state processes. If these processes occur during the time of emission, the lifetime analysis would exhibit a quenched and nonquenched species. Photoionization and charge transfer are two excited-state processes that are pH dependent (Laws & Brand, 1979). Measurements of the lifetimes and emission intensities of DNStyr and the DNStyr derivatives of colipase as a function of pH are presented in Figures 4 and 5. The data points were analyzed by a linear least squares analysis, and the slopes of the ensuing lines were determined. The effect of pH on the first lifetime component of DNStyr is shown in Figure 4A. No significant change was observed. This can be explained by the fact that both the carboxylate and amino groups are blocked. However, either the ionization of the phenolic hydroxyl group is not observed over this pH range or the ionization does not effect DNStyr lifetime. The second lifetime component (data not shown) showed no interpretable pattern and therefore is thought to be random and insignificant. The fluorescence emission of the model compound decreases considerably at very low pH, which may be due to quenching from H_3O^+, but this change is not seen in the lifetime parameters. The $C[1]$ values for both DNStyr55PC and DNStyr59PC showed very gradual increases in lifetime with increasing pH (Figure 5A). The $C[2]$ components for both are relatively unaffected by pH, and the fractional intensities of both are shifted toward $C[2]$ at low pH values. On the whole, no significant changes are observed in the lifetime parameters of DNStyr55PC, DNStyr59PC, and DNStyr as a function of pH. This does not exclude excited-state reactions from operating in a dansyltyrosine system but does indicate that the N- and C-blocked model compound and the dansyltyrosine derivatives of colipase derive double-exponential decay from a mechanism

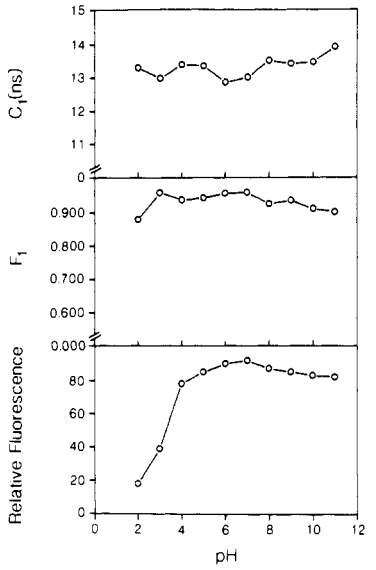

FIGURE 4: Effect of pH on the fluorescence parameters of DNStyr. The concentration of the sample was diluted to $OD_{325nm} < 0.20$ in a 0.05 M K_2HPO_4 buffer adjusted to the appropriate pH. Measurements were made at 24 °C. C_1 is the major lifetime component in the Lorentzian distribution analysis. F_1 is the fractional intensity of the major lifetime component. The relative fluorescence is measured in a steady-state experiment (conditions as in Figure 2).

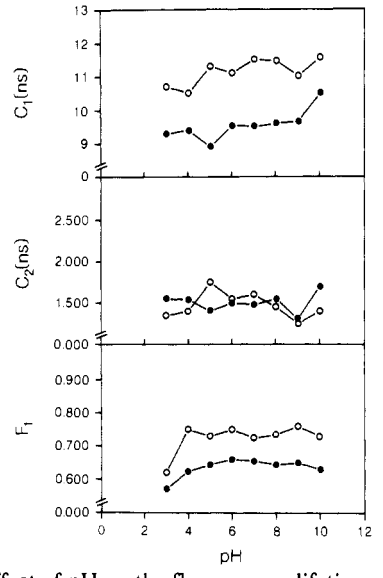

FIGURE 5: Effect of pH on the fluorescence lifetime parameters of DNStyr55PC and DNStyr59PC. In each panel (○) represents DNStyr55PC and (●) represents DNStyr59PC. Sample concentration was diluted to $OD_{325nm} < 0.20$ in a 0.05 M K_2HPO_4 buffer adjusted to the proper pH. C_1 is the major lifetime component; C_2 is the minor lifetime component. F_1 is the fractional intensity of the first component.

other than pH-dependent excited state reactions.

(*b*) *Emission-Resolved Lifetimes of DNStyr and the DNStyr Derivatives of Colipase.* The lifetime of a fluorophore undergoing an excited-state process such as photoionization, charge transfer, or solvent reorientation has a dependence upon the wavelength of emission (Ross et al., 1981). This is due to the existence of continuum of species, undergoing one or more of the previously mentioned processes during the time scale of emission, while others have either not been affected by the process or have completed the process before emission occurs. These species have shifted emission wavelengths relative to each other. The relaxed fluorophores or those that have undergone an excited-state process before emission are red shifted relative to unrelaxed fluorophores (blue edge)

Table III: Emission Resolved Lifetimes[a]

sample	nm	$C[1]$	$F[1]$	$C[2]$	$F[2]$	χ^2
DNStyr (buffer)	475	12.9	0.98	1.5	0.02	20.6
	500	13.1	0.96	1.3	0.04	11.4
	520	13.4	0.95	1.8	0.05	9.3
DNStyr (propylene glycol)	460	14.8	0.96	1.3	0.04	30.8
	500	14.9	0.93	1.8	0.07	14.6
	>530	15.2	0.96	1.9	0.04	4.5
DNStyr55PC	<530	11.6	0.74	1.4	0.26	27.4
	>520	11.9	0.75	1.2	0.25	16.8
	>530	11.8	0.74	1.3	0.26	31.5
	>550	12.0	0.74	1.4	0.26	34.2
DNStyr59PC	<530	9.9	0.68	1.6	0.32	28.4
	>520	9.8	0.67	1.4	0.33	26.7
	>530	10.3	0.68	1.6	0.32	21.9
	>550	10.4	0.69	1.6	0.31	17.1

[a] Lifetimes were obtained under the same conditions as in Table I. The symbols are also described in Table I. Where a single wavelength is indicated, the experiment was done with an emission monochromator. Cut-off filters were used to select wavelength distributions in all other experiments.

(Lakowicz & Cherek, 1980). The result of this phenomena is an increase in mean lifetime across the emission spectrum. The existence of these mechanisms operating in our system have been investigated by measuring lifetime parameters at different wavelengths in the emission spectrum.

Table III shows the analysis of the emission lifetime parameters of DNStyr and DNStyr derivatives of colipase with respect to emission wavelength. The $C[1]$ values for all four samples show minimal increases throughout the emission spectrum. The $C[2]$ values of the modified proteins show no change with emission wavelength, while the $C[2]$ values of DNStyr in buffer and propylene glycol show only slight increases. No significant shifts in the fractional intensities are seen in any sample observed. A two-state excited-state reaction exhibits a definitive wavelength dependence upon emission amplitude and decay kinetics (Ross et al., 1981). The lack of a significant increase in lifetime throughout the emission spectrum argues against these processes operating in the dansyltyrosine colipase system.

(*c*) *Effect of Temperature on the Lifetime Parameters of DNStyr55PC, DNStyr59PC, and DNStyr.* Microheterogeneity in the ground state is a mechanism by which emission decay can be multiexponential. One type of microheterogeneity is the existence of rotational isomers each having unique emission properties. The existence of rotamers can often be examined by their tendency to interconvert due to changes in solvent, temperature, and viscosity (Bartocci et al., 1986). Figure 6 shows the effect of temperature on the lifetime parameters of the compounds being investigated.

The $C[1]$ component of the distribution analysis of DNStyr in buffer decreases gradually with increasing temperature (Figure 6A). The $C[1]$ component of DNStyr in propylene glycol shows no continuing trend throughout the temperature range observed; however, the $C[2]$ component of DNStyr in propylene glycol steadily increases above 30 °C. This increase in the $C[2]$ value is mirrored by an increase in the fractional intensity of the $C[2]$ component. The fraction is steady at about 5% from 5 to 30 °C but then increases to 18% by 50 °C. One possible explanation may be the interconversion of one rotameric species ($C[1]$) to another ($C[2]$). In some cases it is possible that the observed changes are due to an artifact for fitting two lifetimes in which the mean lifetime is becoming shorter. However, fitting the data for both one and two lifetime components showed that the latter is the best fit, further suggesting that the observed changes are real. The $C[2]$ and F values for DNStyr in buffer are not affected by

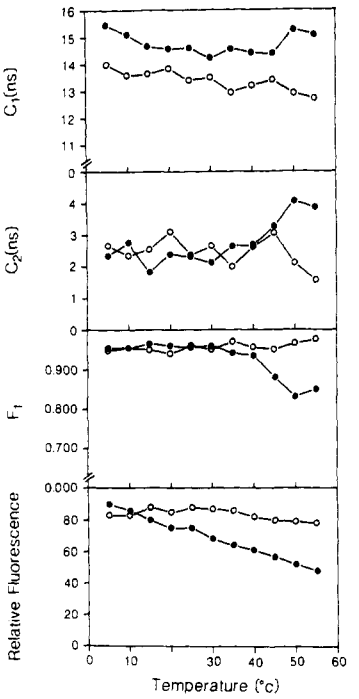

FIGURE 6: Effect of temperature on the fluorescence parameters of DNStyr. Sample concentration was set as described in Figures 3–5. The pH of the 0.05 M K_2HPO_4 buffer was kept at 7.4 at all temperatures. Refer to Figures 4 and 5 for y-axis symbols. In each panel (○) represents DNStyr [buffer] and (●) represents DNStyr [propylene glycol].

temperature. The relative fluorescence of DNStyr in propylene glycol shows a significant decrease in intensity with increasing temperature. Again, DNStyr in buffer shows no effect. This is surprising, as in general fluorophores lose intensity with increasing temperature. This lack of temperature dependence is observed in the lifetime parameters of the model compound in buffer and of the dansyl derivatives of colipase (unpublished data). The effect of temperature on the fluorescence intensity of DNStyr55PC and DNStyr59PC was not determined. The lifetime parameters of both DNStyr55PC and DNStyr59PC are not affected by temperature over the range 5–55 °C.

Discussion

The synthesis and characterization of two unique chemically modified forms of pancreatic porcine colipase are presented. Through a series of nitration, reduction, and dansylation reactions, covalent attachment of a fluorescent probe at tyrosine 55 (DNStyr55PC) and tyrosine 59 (DNStyr59PC) was accomplished. Both steady-state and time-resolved fluorescence spectroscopy were used to characterize the local microenvironments of these two residues. In addition to these studies, experiments on the model compound *N*-acetyl-*o*-aminodansyltyrosine ethyl ester were performed to characterize this probe as a reporter group and to investigate the photophysics of the double-exponential decay of the emission for dansyltyrosine.

The data clearly indicate that Tyr55 is located on the surface of the colipase molecule, free to rotate, as determined by dansyltyrosine fluorescence properties. The emission maximum of 550 nm is highly red shifted for dansyl groups attached to proteins, indicative of a group located in a highly polar solvent. The quenching of the lifetime of DNStyr55PC by the nonionic quencher acrylamide is representative of a fluorophore that is highly accessible to the solvent (unpublished data). Static polarization values derived from differential polarization measurements suggest that the dansyltyrosine 55 group rotates freely by comparison to the model compound and other dansylated derivatives of colipase. A more thorough investigation of the rotational dynamics of DNStyr55PC was accomplished with the use of anisotropy decay experiments. This work shows that the decay of anisotropy for DNStyr55PC is best represented by an anisotropic rotator model with a rotational relaxation rate of 1.0 ns for the fluorophore motion and 4.7 ns for the rotational correlation time of the entire molecule. The acceptance of these values is based on comparisons to anisotropy decay measurements of other proteins in which tryptophan fluorescence was measured. The rotational correlation time of dansyltyrosine in a protein would be expected to be slower than tryptophan due to the larger molecular volume of DNStyr. Gratton et al. have measured rotational correlation times for tryptophan in BPTI and lysozyme; they reported R values no faster than 100 ps, approximately 10 times faster than DNStyr55PC R values (Gratton et al., 1986). The value of 4.7 ns for the rotational tumbling time of colipase is acceptable for a small protein with M_r = 10 500 (Gratton et al., 1986). These anisotropy decay experiments also showed that the *hindered* rotator model does not adequately describe the data, indicating that the angular range of motion of the dansyltyrosine group at residue 55 is unencumbered. The fluorescence characterization of the environment of dansyltyrosine 55 is in agreement with other biophysical and biochemical studies which suggest that one of the three tyrosine residues is on the surface of the protein. Thus, all these studies indicate a highly polar, solvent-exposed environment for this tyrosine, which allows the residue to rotate freely, unhindered by steric constraints. However, in previous studies (Canioni et al., 1980b; Cozzone et al., 1981) it was suggested that either Tyr58 or Tyr59 was the surface tyrosine residue; our data clearly show that tyrosine 55 is on the surface of the molecule.

Tyrosine 59 has been tentatively assigned by NMR and photo-CIDNP as a surface residue. Fluorescence characterization of DNStyr59PC would suggest that Tyr59 is located near the outer surface structure of the protein. Data supporting this possibility are the emission maximum at 520 nm, which indicates a fairly polar environment for the dansyl group attached at Tyr59. More evidence came from acrylamide quenching experiments that showed Tyr55 to be approximately twice as accessible to quencher as Tyr59 (unpublished data). The static polarization value obtained for DNStyr59PC was double the value for DNStyr55PC, assuming modification does not affect the secondary and tertiary structure of the protein. Depolarization due to protein tumbling can be eliminated, thus indicating a more hindered and/or slower rotation for Tyr59 compared to Tyr55. The idea that Tyr59 is located in the outer surface structure is further validated by anisotropy decay data. The *hindered* rotator model best fits the decay of anisotropy for DNStyr59PC. The limiting anisotropy was 0.047, indicative of a fluorophore that experiences hindrance that limits its degree of rotational freedom. All of these data are in agreement with a partially buried location for Tyr59. The fluorescence characterization of DNStyr55PC and DNStyr59PC clearly identifies the microenvironments of Tyr55 and Tyr59 and would suggest that earlier NMR resonance assignments should be reconsidered.

The fluoresence studies of the model compound *N*-acetyl-*o*-aminodansyl tyrosine ethyl ester were designed for two purposes, to characterize the sensitivity of the probe as a reporter group and to investigate possible mechanisms that cause complex emission decay kinetics. An understanding of dansyltyrosine fluorescence would provide important infor-

mation for interpreting studies of the modified proteins with lipid interfaces. By measuring the decay kinetics of DNStyr, DNStyr55PC, and DNtyr59PC under varied conditions, i.e., temperature, solvent, and emission wavelength, along with measuring anisotropy decay parameters, this study has explored the inherent sensitivities of the fluorophore and has developed a model for DNStyr emission decay. The approach taken was to mimic experiments that were used to examine tyrosine and tryptophan photophysics and correlate the results to conclusions in those systems (Beechem & Brand, 1986).

Physical explanations of multiexponential decay kinetics for fluorescence emission can be categorized into two groups. These two groups are ground-state heterogeneity and excited-state processes. Ground-state heterogeneity can arise from several different processes. Discrete protein conformations that would generate two differing microenvironments for the fluorophore are one possible form of ground-state heterogeneity. Multiple excitation transitions that are differentially affected by solvent, temperature, etc. can cause multiple emissions. Rotamers or conformational isomers of the fluorophore each having unique emission properties and microenvironments is yet another type of ground-state heterogeneity (Szabo & Rayner, 1980; Donzel et al., 1974; Gauduchon & Wahl, 1978). Slowly interconverting rotational isomers have been proposed to explain the complex decay kinetics of tryptophan and tyrosine. The nature of the complex photophysics of indole and its derivatives has been studied by many researchers (Valeur & Weber, 1977; Meech et al., 1983; Szabo & Rayner, 1980; Skalski et al., 1980).

Many types of excited-state processes have been shown to be the cause of multiexponential decay kinetics reactions as studied with several different fluorescent molecules. These processes include exciplex formation, charge transfer, electron ejection, photoionization, and solvent or protein reorientation (Beechem & Brand, 1986). These processes involve the interaction of an increased dipole of the excited fluorophore with its surrounding environment and also require that these processes occur on the time scale of emission. It is also possible for more than one mechanism to be associated with multiexponential decay kinetics. It is not within the scope of this paper to attempt to explore each possible mechanism that can cause complex decay kinetics. The goal of this study was to develop a practical model for dansyltyrosine fluorescence that will allow for the use of these probes for biochemical and biophysical studies of colipase and colipase micelle complexes.

Significant insight into tyrosine photophysics has been made by Law and co-workers (Law et al., 1986), who have developed a model for tyrosine decay kinetics based on both NMR and fluorescence data. The use of NMR coupling constants allowed the calculation of the population of the three rotameric isomers about the C_a–C_b bond. These data were correlated with lifetime measurements to allow the following conclusions: They established that photoionization of the phenolic oxygen group did not occur with water in their system and therefore was not a factor in the multiple decay kinetics. They also determined that both exciplex formation and solvent relaxation were not evident. They interpreted their data such that a series of rotational isomer populations were present and that at least one of these rotamers interconverted on a time scale greater than that of emission. These observations can be seen as an argument for rotational isomers being one mechanism by which tyrosine and its derivatives exhibit multiexponential decay kinetics. Investigations of tryptophan, on the other hand, have resulted in a theory that states that different rotamers, each rotating freely at or near the time scale of emission, would experience different microenvironments, causing them to have different decay kinetics.

The absence of a significant pH effect on any of the lifetimes of DNStyr and DNStyr derivatives of colipase suggests that photoionization and charge-transfer reactions are improbable causes of multiexponential decay. The observation that pH does not affect lifetime parameters for DNStyr55PC and DNStyr59PC suggests that ionizable groups are not near these fluorophores or are not interacting with them in a manner that would cause an excited-state reaction. This observation is further validated by emission-resolved-lifetime measurements, which show an insignificant increase in lifetime with longer wavelength. This would rule out the possibility of a two-state excited-state process occurring in the model compound as well as in the modified proteins.

The observation that N- and C-blocked DNStyr has two lifetimes throughout the pH range observed is more in line with tyrosine studies, in which N- and C-blocked Tyr has two and maybe three lifetimes (Law et al., 1986). The rotamer theory as it is applied to Trp, *N*-acetyltryptophanamide, and other derivatives of tryptophan requires that multiexponential decay arise from the interaction of a specific rotamer with neighboring charged groups (Szabo & Rayner et al., 1980). This, however, is not necessary in the case of tyrosine, where, in the absence of a charged group, the rotameric isomers themselves have different rates of decay (Law et al., 1986). This has also been shown to be true for fluorescent molecules lacking ionizable groups, such as styrylnaphthalene, which has two rotamers with lifetimes of 5 and 26 ns (Bartocci et al., 1986). Rotational isomers that orient the naphthalene ring into different microenvironments might explain the differences in the widths of the two lifetime distributions of both DNStyr55PC and DNStyr59PC. The ability to alter external conditions to stimulate the shift from one species to the other would further support the idea that separate populations of rotamers is the principal cause of the two lifetimes of DNStyr derivatives. The shift in fractional intensity of $C[1]$ to $C[2]$ for DNStyr in propylene glycol with increased temperature may represent the interconversion of one species to another.

Naphthalene ring fluorescent derivatives such as dansyl, Prodan, and Acrylodan, which contain diametric substituents with different local charge densities, have large intramolecular charge separation in the excited state. This large excited-state dipole causes these types of fluorophores to be sensitive to local dipolar influences. The fluorescent characteristics of dansyltyrosine are predictably similar to those of Prodan and Acrylodan (Macgregor & Weber, 1986; Prendergast et al., 1983). Dansyltyrosine is sensitive to solvent polarity and viscosity, but is relatively unaffected by pH and temperature (unless temperature alters solvent viscosity significantly). The group also seems to be a reporter of ionic strength (C. Royer, personal communication). Differential solvent quenching efficiencies of the large excited-state dipole of naphthalene-derived fluorophores is another theory that has been embraced to describe complex emission decay kinetics. This may in fact be the cause of multiexponential decay kinetics for dansyltyrosine. However, the experimental approaches taken in this study neither support nor eliminate this possibility.

Aminodansylation of either tyrosine 55 or tyrosine 59 does not eliminate biochemical function and in the case of Tyr55 actually enhances activity. Thus, dansyltyrosine is a sensitive reporter group for solvent polarity and viscosity that does not in this case interfere with protein function. The double-exponential decay of emission for DNStyr derivatives of colipase has been tentatively assigned by a rotamer model on the basis

of experimentation and comparison to tyrosine and tryptophan photophysical studies. However, differential quenching of the large excited-state dipole of the fluorophore cannot be ruled out as an additional mechanism for the complex decay kinetics.

References

Alcala, J. R., Gratton, E., & Prendergast, F. G. (1987a) *Biophys. J. 51*, 587–596.

Alcala, J. R., Gratton, E., & Prendergast, F. G. (1987b) *Biophys. J. 51*, 597–604.

Bartocci, U., Mazzucato, F. M., & Aloisi, G. G. (1986) *Chem. Phys. 101*, 461–466.

Beechem, J. M., & Brand, L. (1985) *Annu. Rev. Biochem. 54*, 43–71.

Caceri, M. S., & Cacheris, W. P. (1980) *Byte 9*, 340.

Canioni, P., & Cozzone, P. J. (1979a) *Biochimie 61*, 353.

Canioni, P., & Cozzone, P. J. (1979b) *FEBS Lett. 97*, 353.

Canioni, P., Julien, R., Rathelot, J., & Sarda, L. (1977) *Lipids 12*, 393.

Canioni, P., Cozzone, P. J., & Kaptein, R. (1980a) *FEBS Lett. 111*, 219.

Canioni, P., Cozzone, P. J., & Sarda, L. (1980b) *Biochim. Biophys. Acta 621*, 29–42.

Cantor, C. R., & Schimmel, P. R. (1980) *Biophysical Chemistry*, Vol. II, p 446, Freeman, San Francisco.

Cardin, A. D., Jackson, R. L., & Johnson, J. D. (1982) *J. Biol. Chem. 257*, 4987–4992.

Chapus, C., Sari, H., Sêmêriva, M., & Desnuelle, P. (1975) *FEBS Lett. 58*, 155.

Chapus, C., Desnuelle, P., & Foglizzo, E. (1981) *Eur. J. Biochem. 115*, 99–105.

Charles, M., Astier, M., Sauve, P., & Desnuelle, P. (1975) *Eur. J. Biochem. 58*, 555.

Charles, M., Sêmêriva, M., & Chabre, M. (1980) *J. Mol. Biol. 139*, 297–317.

Cozzone, P. J. (1976) *FEBS Lett. 69*, 153.

Cozzone, P. J., Canioni, P., Sarda, L., & Kaptein, R. (1981) *Eur. J. Biochem. 114*, 119.

DeCaro, J. D., Behnke, W. D., Bonicel, J. J., Desnuelle, P. A., & Rovery, M. (1982) *Biochim. Biophys. Acta 747*, 253–262.

Donner, J., Spink, C. H., Borgström, B., & Sjoholm, I. (1976) *Biochemistry 15*, 5413.

Donzel, B., Gauduchon, P., & Wahl, P. (1974) *J. Am. Chem. Soc. 96*, 801–808.

Eftink, M. R., & Ghiron, C. A. (1984) *Biochemistry 23*, 3891–3899.

Fiorini, R., Valentino, M., Wang, S., Glaser, M., & Gratton, E. (1987) *Biochemistry 26*, 3864–3870.

Fischer, R. T., Cowlen, M. S., Dempsey, M. E., & Schroeder, F. (1985) *Biochemistry 24*, 3322–3331.

Gauduchon, P., & Wahl, P. (1978) *Biophys. Chem. 8*, 87–104.

Gratton, E., Alcala, J. R., & Marriott, G. (1986) *Biochem. Soc. Trans.*, 617th meeting, Dundee.

Johnson, J. D., Collins, J. H., & Potter, J. D. (1978) *J. Biol. Chem. 253*, 6451–6457.

Kenner, R. A., & Neurath, H. (1971) *Biochemistry 10*, 551–557.

Lakowicz, J. R. (1983) *Principles of Fluorescence Spectroscopy*, Plenum Press, New York.

Lakowicz, J. R., & Cherek, H. (1980) *J. Biol. Chem. 255*, 831–834.

Lakowicz, J. R., Cherek, H., & Balter, A. J. (1981) *Biochem. Biophys. Methods 5*, 131.

Lakowicz, J. R., Laczko, G., Cherek, H., Gratton, E., & Linkeman, M. (1984) *Biophys. J. 46*, 463.

Lakowicz, J. R., Cherek, H., Maliwal, B. P., & Gratton, E. (1985) *Biochemistry 24*, 376–383.

Laws, W. R., & Brand, L. (1979) *J. Phys. Chem. 83*, 795–802.

Laws, W. R., Ross, J. B. A., Wyssbrod, H. R., Beechem, J. M., Brand, L., & Sutherland, J. C. (1986) *Biochemistry 25*, 599–607.

Macgregor, R. B., & Weber, G. (1986) *Nature 319*, 70–73.

McIntyre, J. C., Hundley, P., & Behnke, W. D. (1987) *Biochem. J. 245*, 821–829.

McIntyre, J. C., Schroeder, F., & Behnke, W. D. (1989) *Biophys. J. 55*, 120.

Meech, S. R., Phillips, D., & Lee, A. G. (1983) *Chem. Phys. 80*, 317–328.

Momsen, W. E., & Brockman, H. L. (1976) *J. Biol. Chem. 251*, 378.

Munro, I., Pecht, I., & Stryer, L. (1979) *Proc. Natl. Acad. Sci. U.S.A. 76*, 56–60.

Nemecz, G., & Schroeder, F. (1988) *Biochemistry 27*, 7740–7749.

Prendergast, F. G., Meyer, M., Carlson, G. C., Iida, S., & Potter, J. D. (1983) *J. Biol. Chem. 258*, 7541–7544.

Ross, J. B. A., Rousslag, K. W., & Brand, L. (1981) *Biochemistry 20* 4361–4369.

Sari, H., Entressangles, B., & Desnuelle, P. (1975) *Eur. J. Biochem. 58*, 561–565.

Schroeder, F., Barenholz, Y., Gratton, E., & Thompson, T. E. (1987) *Biochemistry 26*, 2441–2447.

Skalski, B., Rayner, D. M., & Szabo, A. G. (1980) *Chem. Phys. Lett. 70*, 587–590.

Smyth, D. G., Nagamatsu, A., & Fruton, J. S. (1968) *J. Am. Chem. Soc. 82*, 4600–4604.

Sokolovsky, M., Riordan, J. F., & Vallee, B. L. (1966) *Biochemistry 5*, 3582–3589.

Sokolovsky, M., Riordan, J. F., & Vallee, B. L. (1967) *Biochem. Biophys. Res. Commun. 27*, 20–25.

Sweet, W. D., Wood, W. G., & Schroeder, F. (1987) *Biochemistry 26*, 2828–2834.

Szabo, A. G., & Rayner, D. M. (1980) *J. Am. Chem. Soc. 102*, 554.

Szabo, A. G., Stepanik, T. M., Wayner, D. M., & Young, N. M. (1983) *Biophys. J. 41*, 233.

Valeur, B., & Weber, G. (1977) *Photochem. Photobiol. 25*, 441–444.

Verger, R., Rietsch, J., & Desnuelle, P. (1977) *J. Biol. Chem. 252*, 4319.

Wieloch, T., & Falk, K. E. (1978) *FEBS Lett. 85*, 271.